

SIMULATION OF FEEDFORWARD CONTROL TECHNIQUES TO IMPROVE MACHINES FEED DRIVES TRACKING PERFORMANCE

J. Ferkl^{1*}, L. Novotny¹, X. Beudaert², O. Franco², P. Kolar¹

¹ Czech Technical University in Prague, Faculty of Mechanical Engineering, Department of Production Machines and Equipment, Prague, Czech Republic

² Dynamics & Control Department, Ideko, Elgoibar, Basque Country, Spain

*Corresponding author; e-mail: j.ferkl@rcmt.cvut.cz

Abstract

High speed machines such as laser cutting machines should realize movements with high accelerations. Dynamical limitations of the feed drives are typically related to the bandwidth of the control loops and the excitation of mechanical structure. The objective of this article is to analyze the effect of feedforward control techniques on the individual axes tracking performance. Feed drive simulation model of increasing complexity is developed and valid relations between tracking performance and applied feedforward techniques are described. Consequently, this paper offers contribution in terms of feedforwards tuning, modelling and determination of achievable improvements and limitations.

Keywords:

Feedforward, High Speed Machine, Simulation, Feed Drive

1 INTRODUCTION

In the present manufacturing industry, the demand for high speed and high accuracy is constantly growing. The sources of inaccuracy can be decomposed in quasi-static geometric error which are independent of the feedrate like geometric or thermal errors and the dynamical geometric errors. When the feed is increased the dynamical errors can represent a significant contribution of the total contouring errors as measured by Andolfatto et al. [Andolfatto 2011]. Indeed, first, high accelerations and decelerations generate inertial loads which excite the vibration modes of the machine. Second, high feedrate generates high following control errors. And last but not least, during high speed multi-axis interpolation the dynamical synchronization of the different axes become crucial. Hence, a perfect accuracy at low feed can be ruined at high speed due to a poor tuning of the feed drive controllers.

In feedback control, actuating signal is a controller's reaction to a control error. Thus, difference between reference and actual signal has to manifest first before the controller reacts. Such a robust control law has its limitations in terms of tracking performance. These can be exceeded by feedforward control (FFW). The term has several different meanings. In the field of machine tools and production machines, there are following established concepts (Fig. 1): modulation of reference signal a priori the

closed control loops ('Pilot control', Fig. 1 a), [Brecher 2022]) and bypassing the feedback controller ('Parallel feedforward element', Fig. 1 c), [Brecher 2022]). The aim of both techniques is to improve the tracking performance of the feedback control law.

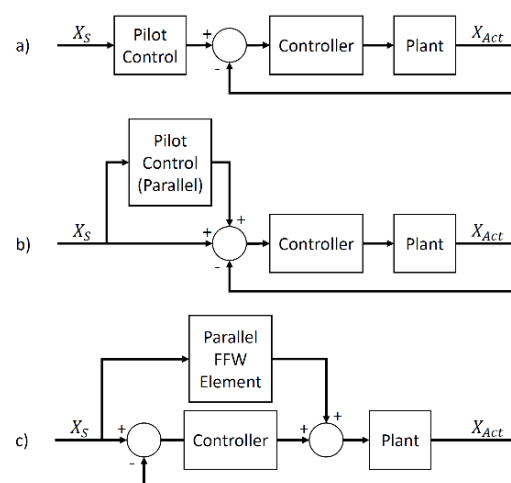


Fig. 1: Different FFW types

Pilot control (Fig. 1 a)) technique is based on filtering the reference signal with the inverse function of the whole feedback loop. This ideally results in unit transfer function between actual position and reference. Practically, there are three obstacles: causality, robustness and stability. Causality isn't crucial as the G-code is typically completely known. Robustness (quality of mathematical description of the closed control loop) and stability of the inversed term are the usual shortcoming. Well received 'Zero Phase Error Tracking Control' (ZPETC) [Tomizuka 1987] addresses the problem of the stability by dividing zeroes into stable and unstable. Stable zeroes are easily inversed and the phase error caused by the unstable zeroes are compensated by additional noncausal term. Weck et al. [Weck 1990] proposed the 'Inverse compensation filter'. It enhances the tracking performance of the ZPETC in the sharp corners by lowpass filtering the original reference signal.

Discussed Pilot control technique filters the reference signal directly in the input channel of the system. Alternatively, compensation of the dynamical behavior of the control loop can be achieved by superposing original reference signal with the outputs of the compensation filters in parallel connection (Fig. 1 b)). Fanuc patent [Wang 2018] introduces additional position command. It is calculated by 'learning control unit' based on position reference signal. Parameters of this modulation are optimized utilizing accelerometer located near the positioned endpoint. Dumanli et al. [Dumanli 2019] proposed linear dynamics and friction compensation filters with parameters identified using optimization directly on the machine. The parameters of the simplified mathematical description are identified based on the contour error minimization.

Parallel FFW (Fig. 1 c)) bypasses the feedback controller and feeds the additional reference signal inside the control loop. In case of the P-PI-PI (position, velocity and current) cascade controller, the velocity FFW (bypasses position controller) and current FFW (bypasses position and velocity controller) are the most utilized techniques. Bypassing the innermost current controller is typically not applied as the reference signal quality requirements would increase rapidly with respect to the bandwidth.

Velocity and current FFWs input the reference trajectory inside the cascade controller in form of additional reference signals. Ideally, the bypassed controller action is completely substituted by the FFW as there is no control error (of the bypassed controller). This is typically not achievable as the feedback signal is influenced by the controlled system dynamics and disturbances. Thus, discrepancies between reference and feedback signals occur. As a result of the discrepancies, the two reference signals do not cancel each other out completely and the overshoots are formed. This issue is typically addressed by lowering the weighting factor of the FFW. An alternative within the Siemens Sinumerik control system are so-called balancing filters [Siemens 2023] [Gross 2001]. The general idea is to approximate the controlled system dynamics with a lowpass filter and use it on the bypassed controller reference signal. Ideally, both reference and feedback signals are affected by the same dynamical behavior of the controlled system and the result of the subtraction is once again approaching zero. This corresponds to the aforementioned ideal FFW state. Limitations of this technique will be further discussed in section 2.

Heidenhain TNC 640 control system features the function called 'jerk feedforward control' [Heidenhain 2020]. The term is further discussed in the Heidenhain patent [Kerner 2000]. Despite this fact, it's working principle is not completely clear. As will be further discussed in the chapter

2, applying the jerk signal of the reference trajectory as additional velocity command compensates the following error during changes in acceleration.

Inner control loops of the cascade controller have a higher bandwidths and therefore usually run at lower cycle time. Thus, the quality requirements for the reference signal increases. Poor sampling frequency and resolution of the reference signal result in system behavior similar to step response. Modern control systems are capable of reference and feedback signal resolution up to 0.1 nm [Fanuc 2017]. Siemens Sinumerik control system offers so called "Dynamic Servo Control". The function addresses the described problem with the help of the additional interpolation between position and velocity controllers and the additional position controller running at velocity control loop cycle time [Siemens 2005].

Many compensation functions of modern control systems are based on feedforwards working principle: friction, vertical axis weight, torsion, backlash... Typically, there is a reference model of the compensated phenomenon whose parameters are identified experimentally with the help of optimization task. Matsubara et al. [Matsubara 2011] proposed Model-Reference feedforward controller which inputs the reference signal of all three control loops through the reference model of the controlled system. Fanuc control systems feature 'AI Feedforward' [Fanuc 2018] whose working principle is (probably) disclosed in the patent [Tsuneki 2020]. It combines pilot control and the parallel FFWs. The aim is to compensate low frequency mechanical oscillations. Therefore, the filters parameters are identified with the help of an accelerometer which is located near the tool center point and is installed only during initial optimization. Potentially, this technique is capable of suppressing the mechanical oscillations outside the closed position control loop.

To the best of the author's knowledge, no previous published work offers a comprehensive examination of aforementioned FFWs techniques. In this paper, sequential modeling approach is used to define the valid relations and limitations. The starting point is a transparent and most simplified model of dynamical behavior. This ideal state allows to achieve unrealistically good tracking performance. Subsequently, the simulation models of increasing complexity of the controlled system are examined. This allows to understand the optimal control parameters tuning, valid technical constraints and required simulation model complexity to achieve realistic simulation results.

The rest of this paper is organized as follows: in section number 2, different feedforward techniques are examined and simulated. Tuning of the corresponding parameters is discussed. The feedforward techniques are evaluated based on the tracking performance of the individual axis. Next, the results are discussed and summarized.

2 VELOCITY AND ACCELERATION FEEDFORWARD CONTROL TECHNIQUES

In this section, the simulation models of increased complexity are developed to examine the relations between controlled system properties and achievable results by utilizing different FFW techniques. This approach offers guidelines for FFW parameters tuning and also insight into applicability of the discussed techniques. The simulation models are available at [Ferkl 2023] as open source files. Reference trajectory is generated with the help of the jerk generator [Lambrechts 2023] and integration to acceleration/velocity/position (Fig. 3). The same motion profile was used for all simulations (Fig. 2, Tab. 1).

Tab. 1: Reference trajectory parameters

max. jerk [m/s ³]	1000
max. acceleration [m/s ²]	20
max. velocity [m/s]	3.33
target position [m]	2

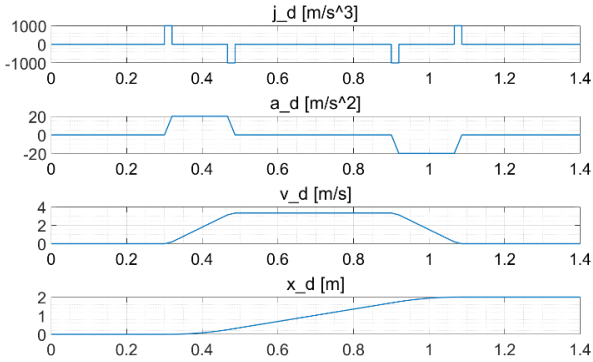


Fig. 2: Reference trajectory

2.1 Velocity control loop PT1 approximation

The first dynamical model of the feed axis that allows to study the effect of parallel FFW element approximates the velocity control loop with a 1st order low pass filter, considering following general block diagram (Fig. 3).

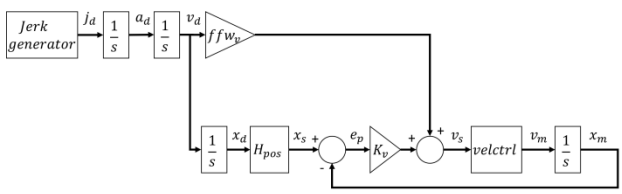


Fig. 3: Block diagram of feed axis model with approximated velocity control loop

The transfer function between demanded velocity (v_d) and position error (e_p) can be expressed (1) as a function of reference position signal filter H_{pos} , velocity FFW weighting factor ffw_v , closed velocity control loop $velctrl$ and position proportional controller gain K_v .

$$\frac{e_p}{v_d} = \frac{H_{pos} - ffw_v * velctrl}{s + K_v * velctrl} \quad (1)$$

A 1st order low pass filter is assigned to the velocity control loop transfer function (2).

$$velctrl = \frac{1}{1 + \tau_{velctrl} * s} \quad (2)$$

H_{pos} filters the position control loop reference signal x_d . The filtering can be turned off by assigning the unit transfer function (3).

$$H_{pos} = 1 \quad (3)$$

DC gain of resulting transfer function $\frac{e_p}{v_d}$ can be expressed (4).

$$\lim_{s \rightarrow 0} \left(\frac{e_p}{v_d} \right) = \frac{1 - ffw_v}{K_v} \quad (4)$$

For $ffw_v = 1$ the position error at constant velocity is zero. Feedforward influence can be observed during point-to-point positioning of a feed axis (Fig. 4). For this purpose, numeric values of model parameters have to be assigned. Bandwidth of the closed velocity loop $f_{bw\ vel}$ was selected.

Based on this value, the model parameters were calculated (Tab. 2).

Tab. 2: PT1 model parameters

$f_{bw\ vel}$ [Hz]	70
K_v [1/s]	110
$\tau_{velctrl}$ [s]	$2.27e - 3$

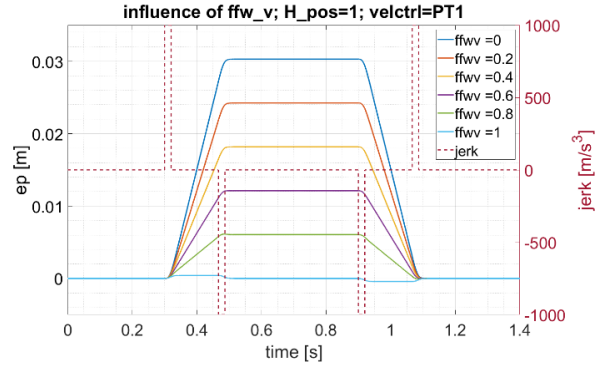


Fig. 4: Position error during point to point motion – influence of ffw_v ; velocity control loop approximated as a 1st order low pass filter

For $ffw_v = 1$, the position error is significantly lowered. It is zero only at constant velocity (and during motion reversals) (Fig. 5).

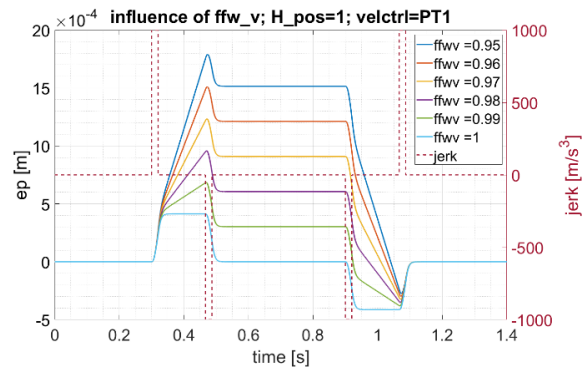


Fig. 5: Position error during point to point motion – influence of ffw_v (detail); velocity control loop approximated as a 1st order low pass filter

This motivates the implementation of the H_{pos} filter. In the Siemens Sinumerik control system, the filter is referred to as ‘balancing filter’ and it is defined as the first order low pass filter [Siemens 2023] [Gross 2001]. In this simplified example, $velctrl$ and H_{pos} have the same structure. With correct parametrization, the two subtracted signals can be matched perfectly (Fig. 6).

This corresponds to the ideal FFW state as $e_p = 0$. It comes at the expense of the low pass filtering of the position loop reference signal. It can be analytically shown that for $H_{pos} = velctrl$ and $ffw_v = 1$ the transfer function $\frac{x_m}{x_d} = velctrl$ (5).

$$\frac{x_m}{x_d} = velctrl * \frac{K_v * H_{pos} + ffw_v * s}{K_v * velctrl + 1 * s} \quad (5)$$

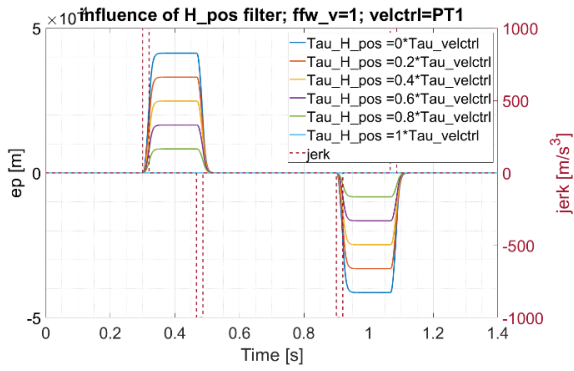


Fig. 6: Position error during point to point positioning – influence of H_{pos} ; velocity control loop approximated as a 1st order low pass filter

2.2 Velocity control loop PT2 approximation

As previously mentioned, the H_{pos} filter is in Sinumerik control system defined as a 1st order low pass filter. A 2nd order low pass filter approximation of the velocity control loop is the most transparent possibility to examine the effects of a different dynamics between H_{pos} and $velctrl$. The block diagram (Fig. 3) remains valid. The numeric values were once again determined based on the velocity control loop bandwidth $f_{bw\ vel}$ selection (Tab. 3).

Tab. 3: PT2 model parameters

$f_{bw\ vel}$ [Hz]	70
K_v [1/s]	110
D_{vel} [-]	$\sqrt{2}/2$
ω_{vel} [rad/s]	440

The 2nd order low pass filter is assigned to the velocity control loop transfer function (6). The H_{pos} is initially turned off (3). Value lower than 1 is assigned to the damping ratio parameter D_{vel} which results in oscillatory behavior. The ω_{vel} parameter represents undamped natural angular velocity of the system. Bandwidth of the 2nd order velocity control loop approximation is matched with the bandwidth of the 1st order approximation.

$$velctrl = \frac{1}{\frac{s^2}{\omega_{vel}^2} + \frac{2 * D_{vel} * s}{\omega_{vel}} + 1} \quad (6)$$

The expression (4) remains valid as the position error is zero at constant velocity in case of $ffw_v = 1$ (Fig. 7).

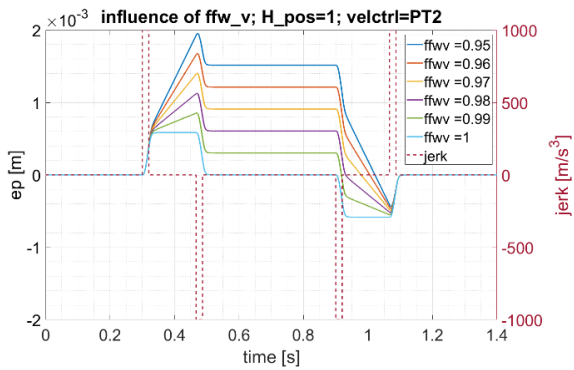


Fig. 7: Position error during point to point motion – influence of ffw_v ; $H_{pos}=1$; $velctrl=PT2$ as a 2nd order low pass filter

It can be seen that the position error stabilizes during constant acceleration phase at a constant value. The static component of the position error can be further suppressed with the help of H_{pos} (Fig. 8).

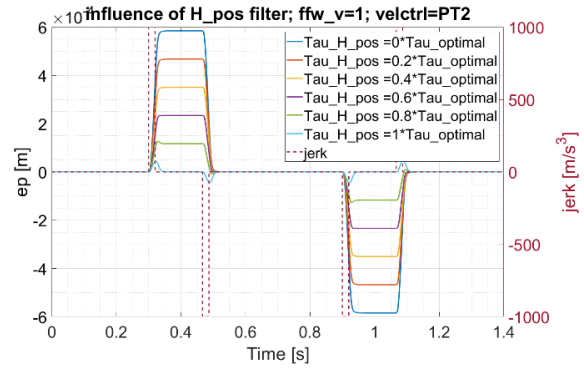


Fig. 8: Position error during point to point positioning – influence of H_{pos} ; velocity control loop approximated as a 2nd order low pass filter

Optimal parametrization of H_{pos} can be expressed analytically (7) with the help of DC gain.

$$\lim_{s \rightarrow 0} \left(\frac{e_p}{a_d} \right) = 0 \rightarrow \tau_{H_{pos}\ optimal} = \frac{2 * D_{vel}}{\omega_{vel}} \quad (7)$$

Transient effects during change of acceleration can't be compensated completely as the H_{pos} and $velctrl$ features different dynamical behavior (Fig. 9).

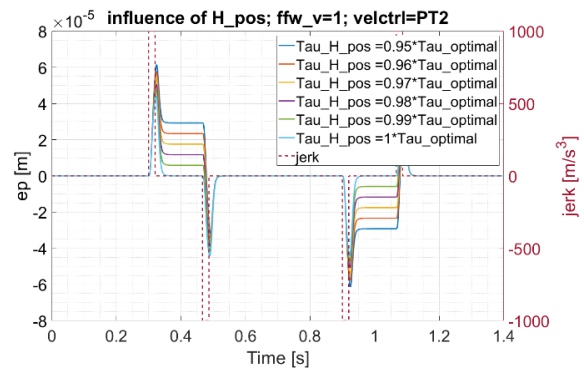


Fig. 9: Position error during point to point positioning – influence of H_{pos} (detail); velocity control loop approximated as a 2nd order low pass filter

2.3 1-DOF mechanics

In the previous sections the velocity control loop was approximated with low pass filters. Next, the feedback control loop is considered (Fig. 10). The parameter m represents positioned mass. K_f is a force constant, which describes proportionality between motor current and resulting force. The transfer function $velreg$ stands for PI velocity controller with proportional gain K_{pv} and integral time T_n (8).

$$velreg = K_{pv} * \frac{T_n * s + 1}{T_n * s} \quad (8)$$

For simplicity, the current control loop is initially approximated as a unit transfer function. The model is still linear and can be assigned to a single transfer function $velctrl$ of the block diagram (Fig. 3).

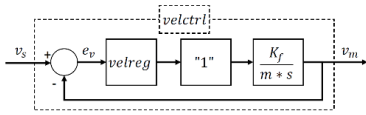


Fig. 10: Velocity feedback loop

The numeric values were once again calculated based on the closed velocity control loop bandwidth $f_{bw\ vel}$ (Tab. 4). For this purpose, formulas presented in the thesis [Franco 2021] were used (9) (10) (11).

$$K_{pv} = \frac{2 * \pi * m * f_{bw\ vel}}{K_f} \quad (9)$$

$$T_n = \frac{1}{\pi * f_{bw\ vel}} \quad (10)$$

$$K_v = \frac{\pi * f_{bw\ vel}}{2} \quad (11)$$

Tab. 4: Feedback 1DOF model parameters

$f_{bw\ vel}$ [Hz]	70
K_v [1/s]	110
K_{pv} [A/(m/s)]	6.16e4
T_n [s]	4.55e-3
m [kg]	140
K_f [N/A]	1

Initially, let's consider integral controller turned off. For proportional controller, the control loop transfer function corresponds to a 1st order low pass filter examined in section 2.1. The resulting time constant can be derived and used for H_{pos} parametrization (12).

$$\tau_{P\ velreg} = \frac{m}{K_{pv} * K_f} \quad (12)$$

In case of proportional-integral controller, the behavior differs significantly. With $ffw_v = 1$, the static component of position error is zero during constant velocity phase as well as during constant acceleration phase of the reference motion (Fig. 11).

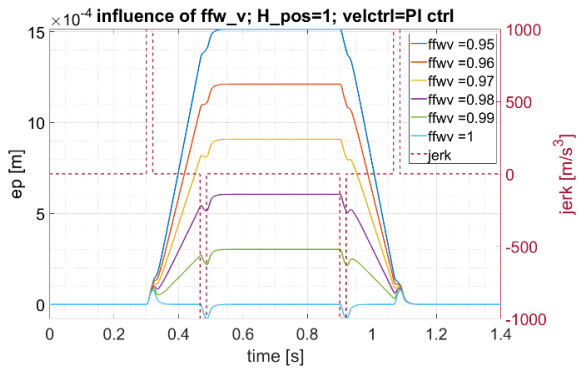


Fig. 11: Position error during point-to-point motion – influence of ffw_v ; velocity proportional-integral control

Consequently, there is no need for H_{pos} filter (13). It would influence the resulting position error negatively (Fig. 12).

$$\lim_{s \rightarrow 0} \left(\frac{e_p}{a_d} \right) = 0 \rightarrow \tau_{H_{pos}\ optimal} = 0 \quad (13)$$

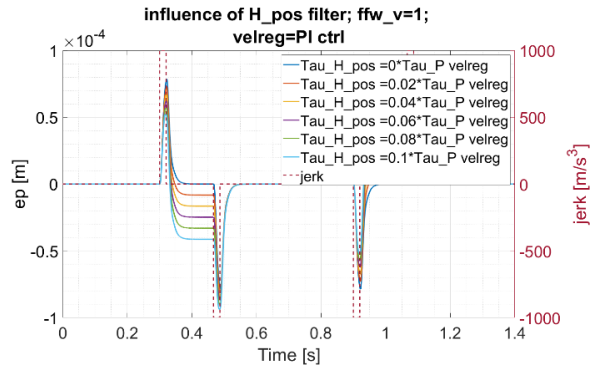


Fig. 12: Position error during point to point motion – influence of H_{pos} ; $ffw_v = 1$; velocity proportional-integral control

On the other hand, the DC gain $\frac{e_p}{j_d}$ isn't zero. Thus, jerk reference signal j_d (Fig. 2) multiplied by weighting factor ffw_v can be introduced as an additional velocity feedforward (Fig. 13). This functionality is known as 'jerk feedforward' [Heidenhain 2020] [Kerner 2000].

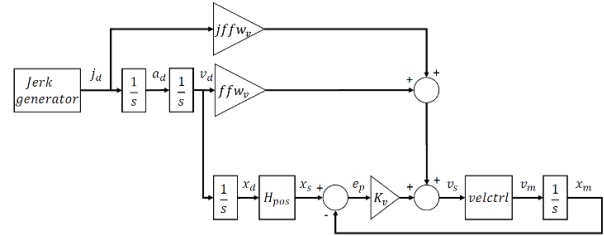


Fig. 13: Block diagram of feed axis model with jerk FFW

Optimal parametrization of the jerk FFW weighting factor ffw_v can be expressed with the help of DC gain equal to zero (14).

$$\lim_{s \rightarrow 0} \left(\frac{e_p}{j_d} \right) = 0 \rightarrow ffw_v\ optimal = \frac{T_n * m}{K_f * K_{pv}} \quad (14)$$

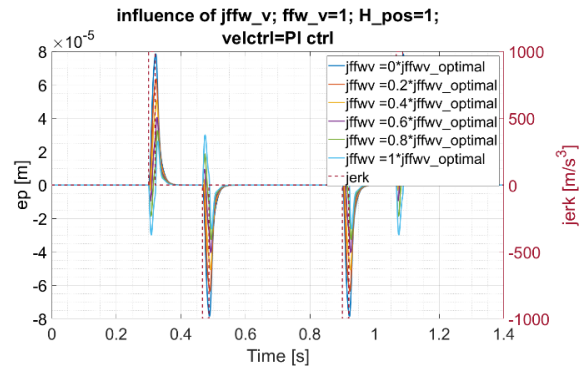


Fig. 14: Position error during point to point motion – influence of jfw_v ; velocity proportional-integral control

Feeding forward jerk reference signal shaped as pulses results in step response behavior and overshoots (Fig. 14). This problem can be further addressed with the help of lowpass filtering in the jerk FFW branch.

Velocity control loop modeled as a feedback loop allows to examine effects of acceleration FFW (Fig. 16). Besides the new FFW branch, a 1st order low pass filter H_{vel} is introduced. Theoretically, it allows to achieve the ideal acceleration FFW state as the bypassed controllers' errors are zero ($e_p = e_v = 0$, Fig. 15).

$$ffw_v = 1 \quad (15)$$

$$ffw_a = \frac{m}{K_f} \quad (16)$$

$$H_{pos} = currctrl \quad (17)$$

$$H_{vel} = currctrl \quad (18)$$

The fraction in equation (19) equals one in case of optimal parametrization (15)(16)(17)(18). As a result, the transfer function between x_d and x_m is equal to the transfer function of the closed current loop $currctrl$. In Siemens Sinumerik control system, the H_{pos} and H_{vel} filters are defined as 1st order low pass filters [Siemens 2023]. Presented parametrization and results are valid only for absolutely rigid mechanical structure (1DOF) and $currctrl$ behaving like a 1st order lowpass filter (Tab. 5).

Tab. 5: Feedback 1DOF model parameters

$f_{bw\ currctrl}$ [Hz]	1000
$\tau_{currctrl}$ [s]	$1.59e - 4$

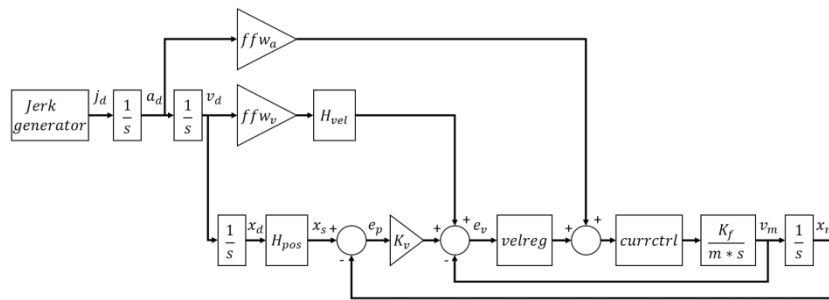


Fig. 16: Block diagram for acceleration FFW simulations

$$\frac{x_m}{x_d} = currctrl * \frac{s^2 * ffw_a * K_f + s * velreg * H_{vel} * K_f * ffw_v + velreg * H_{pos} * K_v * K_f}{s^2 * m + s * velreg * currctrl * K_f + velreg * currctrl * K_v * K_f} \quad (19)$$

3 DISCUSSION

In this paper, different feedforward control techniques are utilized on the feed axis models of increasing complexity. Elementary relations are examined and analytically expressed. For this purpose, simplified models of dynamical behavior are considered. Achieved results are further to be utilized in case of more complex mathematical models and real-world feed axes, where analytical approach is not possible. Despite this fact, elementary constrains described in this article are going to be valid and used as foundations.

Future work is required (Fig. 17) to address the topic of mechanical compliance inside and outside of the closed position control loop. Different source of velocity feedback and position feedback in case of direct measuring system is possibly another technical challenge to consider. Discrete control and nonlinear dynamical behavior such as friction and backlash also affect achievable tracking performance especially during motion reversals. These phenomena are not considered in this work.

The tool center point trajectory is a result of individual axes motions. Different axes bandwidths result in geometry errors due to poor axes synchronization. The topic is directly related to the tracking performance of individual axes and thus feedforwards. It presents another research opportunity.

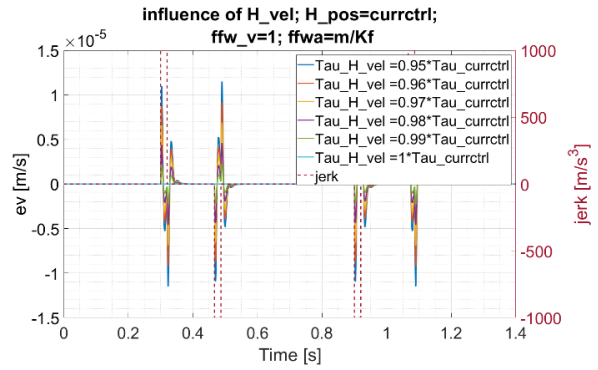


Fig. 15: Velocity error during point to point motion – influence of H_{vel} ; velocity proportional-integral control; $ffw_v = ffw_a = 1$; $H_{pos} = currctrl$

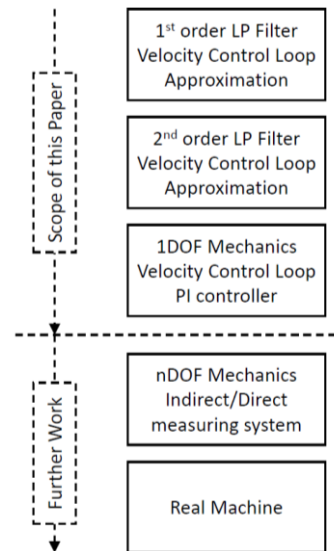


Fig. 17: Scope of this paper

In section 2.3, the influence of the H_{pos} filtering was examined in case of P and PI velocity controller. Positive influence is observed only in case of P velocity controller. Thus, so called 'balancing filters' are typically not applied in case of standard P-PI-PI cascade control. Their importance is related to the application of closed velocity loop with reference model. [Siemens 2021] [Heidenhain 2020] [Gross 2001] [Kerner 2000] The technique allows the velocity controller to act like a P controller with respect to tracking

performance and like a PI controller with respect to disturbance rejection. This results in enhanced tracking performance that can be further improved with filtering examined in this work.

4 SUMMARY

This article offers extensive research of feedforward techniques present in the modern control systems. Among others, the velocity and current parallel feedforwards are the most established. Despite this fact, no previous work offers in depth insight into application guidelines, technical constraints and relations to other relevant feed drives control techniques. To explore mentioned topics, simulation models of increasing complexity were developed.

Ideal state was described in case of velocity FFW as well as in case of acceleration FFW. Subsequently, the examined conditions were further complicated. Optimal FFW parametrization was derived with the help of zero DC gain between reference velocity/acceleration/jerk and control error of the bypassed controller. Namely, effects of ffw_v , ffw_a , $\tau_{H_{pos}}$ and $\tau_{H_{vel}}$ were examined in case of a 1st and a 2nd order low pass filter approximation of the velocity control loop and also in case of feedback loop with 1DOF mechanics.

5 ACKNOWLEDGMENTS

The presented results were created with the knowledge contribution gained thanks to previous funding support from the Czech Ministry of Education, Youth and Sports under the project CZ.02.1.01/0.0/0.0/16_026/0008404 "Machine Tools and Precision Engineering" financed by the OP RDE (ERDF) and co-funded by the European Union. The contribution of the Ph.D. student involved in the author team was also supported by the Grant Agency of the Czech Technical University in Prague, grant no. SGS22/159/OHK2/3T/12. This research has been also partially funded by the LaserStarLine Eurostars project.

6 REFERENCES

[Andolfatto 2011] Andolfatto, L., Lavernhe, S., & Mayer, J. R. R. (2011). Evaluation of servo, geometric and dynamic error sources on five-axis high-speed machine tool [Online]. International Journal Of Machine Tools And Manufacture, 51(10-11), 787-796. <https://doi.org/10.1016/j.ijmachtools.2011.07.002>

[Brecher 2022] Brecher, C., & Weck, M. (2022). Machine Tools Production Systems 3 [Online]. Wiesbaden: Springer Fachmedien Wiesbaden. <https://doi.org/10.1007/978-3-658-34622-5>

[Dumanli 2019] Dumanli, A., & Sencer, B. (2019). Pre-compensation of servo tracking errors through data-based reference trajectory modification [Online]. Cirp Annals, 68(1), 397-400. <https://doi.org/10.1016/j.cirp.2019.03.017>

[Fanuc 2017] Fanuc. (2017). FANUC ROBOTONANO α -NTiA: Ultra precision, enhanced ease of use and sustainability. Retrieved from <https://one.fanuc.eu/l/442582/2021-09-20/c1yp2q>

[Fanuc 2018] FANUC CORPORATION. (2018). AI Feedforward SPECIFICATION MANUAL. Retrieved from <https://my.fanuc.eu/>

[Ferkl 2023] Ferkl (2023). SIMULATION OF FEEDFORWARD CONTROL TECHNIQUES <https://www.mathworks.com/matlabcentral/fileexchange/1>

[31329-simulation-of-feedforward-control-techniques](https://www.mathworks.com/matlabcentral/fileexchange/131329-simulation-of-feedforward-control-techniques), MATLAB Central File Exchange. Retrieved June 19, 2023.

[Franco 2021] Franco Dobaran, Oier (2021). Influence of feed drives on the structural dynamics of large-scale machine tools. University Of Waterloo. <https://doi.org/http://hdl.handle.net/10012/17819>

[Gross 2001] Groß, H., Hamann, J., Wiegärtner, G., & Aktiengesellschaft, S. (2001). Electrical Feed Drives in Automation: Basics, Computation, Dimensioning: Basics, Computation, Dimensioning. Wiley. ISBN 3895781487.

[Heidenhain 2020] HEIDENHAIN. (02/2020AD). TNC 640 Technical Manual: NC Software 34059x-10. Traunreut, Germany. Retrieved from <http://portal.heidenhain.de>

[Kerner 2000] KERNER, Norbert. DR. JOHANNES HEIDENHAIN GMBH. Method for determining time constants of a reference model in a cascade controlling circuit. USOO69 12426B1. US. Sep. 21. 2000.

[Lambrechts 2023] Lambrechts (2023). Advanced Setpoints for Motion Systems <https://www.mathworks.com/matlabcentral/fileexchange/16352-advanced-setpoints-for-motion-systems>, MATLAB Central File Exchange. Retrieved May 25, 2023.

[Matsubara 2011] Matsubara, A., Nagaoka, K., & Fujita, T. (2011). Model-reference feedforward controller design for high-accuracy contouring control of machine tool axes [Online]. Cirp Annals, 60(1), 415-418. <https://doi.org/10.1016/j.cirp.2011.03.029>

[Siemens 2005] Siemens AG. (2005). 1-2SEB3E_DSC-Regelung.doc. Retrieved from https://cache.industry.siemens.com/dl/files/144/22057144/att_113106/v1/dsc-regulation.pdf

[Siemens 2021] Siemens. Drive Optimization Guide: Guideline for drive optimization of servo motors with SINAMICS S120, S210 and V90, 2021. <https://doi.org/https://support.industry.siemens.com/cs/document/60593549/drive-optimization-guide?dti=0&lc=en-KR>

[Siemens 2023] Siemens. (2023). SINUMERIK ONE axes and spindles: A5E48053595B AG. Retrieved from <https://support.industry.siemens.com/cs/document/109817116/sinumerik-one-axes-and-spindles?dti=0&lc=en-KR>

[Tomizuka 1987] Tomizuka, M. (1987). Zero Phase Error Tracking Algorithm for Digital Control [Online]. Journal Of Dynamic Systems, Measurement, And Control, 109(1), 65-68. <https://doi.org/10.1115/1.3143822>

[Tsuneki 2020] TSUNEKI, Ryoutarou. FANUC CORPORATION. Machine learning device, control system, and machine learning. US011243501B2. 2020.

[Wang 2018] WANG, Kaimeng. FANUC CORPORATION. Robot system having learning control function and learning control method. US 20180229364A1. Feb. 9. 2018.

[Weck 1990] Weck, M., & Ye, G. (1990). Sharp Corner Tracking Using the IKF Control Strategy [Online]. Cirp Annals, 39(1), 437-441. [https://doi.org/10.1016/S0007-8506\(07\)61091-9](https://doi.org/10.1016/S0007-8506(07)61091-9)